

Development of a nanosecond-laser-pumped Raman amplifier for short laser pulses in plasma

Y. Ping,¹ R. K. Kirkwood,¹ T.-L. Wang,² D. S. Clark,¹ S. C. Wilks,¹ N. Meezan,¹ R. L. Berger,¹ J. Wurtele,³ N. J. Fisch,⁴ V. M. Malkin,⁴ E. J. Valeo,⁴ S. F. Martins,² and C. Joshi²

¹*Lawrence Livermore National Laboratory, Livermore, California 94550, USA*

²*Department of Electrical Engineering, University of California at Los Angeles, Los Angeles, California 90095, USA*

³*Department of Physics, University of California at Berkeley, Berkeley, California 94720, USA*

⁴*Department of Astrophysical Sciences, Princeton University, Princeton, New Jersey 08544, USA*

(Received 13 August 2009; accepted 3 December 2009; published online 31 December 2009)

Progress on developing a plasma amplifier/compressor based on stimulated Raman scattering of nanosecond laser pulses is reported. Generation of a millijoule seed pulse at a wavelength that is redshifted relative to the pump beam has been achieved using an external Raman gas cell. By interacting the shifted picosecond seed pulse and the nanosecond pump pulse in a gas jet plasma at a density of $\sim 10^{19}$ cm⁻³, the upper limit of the pump intensity to avoid angular spray of the amplified seed has been determined. The Raman amplification has been studied as a function of the pump and seed intensities. Although the heating of plasma by the nanosecond pump pulse results in strong Landau damping of the plasma wave, an amplified pulse with an energy of up to 14 mJ has been demonstrated, which is, to the best of our knowledge, the highest output energy so far by Raman amplification in a plasma. One-dimensional particle-in-cell simulations indicate that the saturation of amplification is consistent with onset of particle trapping, which might be overcome by employing a shorter seed pulse. © 2009 American Institute of Physics. [doi:10.1063/1.3276739]

I. INTRODUCTION

Raman amplification of short laser pulses in a plasma was proposed a decade ago in order to reach ultrahigh laser powers well above that currently available by chirped pulse amplification laser systems.^{1,2} This Raman scheme utilizes plasma as the gain medium to overcome the limit imposed by the damage threshold of solid-state optics. The amplification of short laser pulses is achieved by energy transfer from a long pump pulse through a three-wave interaction with a plasma wave. The interaction can be either resonant by matching the frequency difference of the pump and the seed with the plasma frequency² or nonresonant if the pump and the seed pulses are intense enough to drive a transient plasma density perturbation, which scatters the energy from the pump to the seed, so called the superradiant regime.¹ Since the first experimental demonstration of Raman amplification of a short laser pulse in a plasma,³ there has been a growing interest in developing a plasma amplifier and compressor for short laser pulses in both theoretical⁴⁻⁹ and experimental¹⁰⁻¹⁷ studies. Recent experiments have demonstrated compression of the amplified pulse from 500 fs to 150 fs by a 30 mJ, 10 ps pump pulse.¹³ The interaction length has been extended by double-pass (~ 4 mm) (Ref. 15) or waveguiding (~ 9 mm) (Ref. 16) to reach higher output energy, making the plasma amplifier close to a practical device.

At present most experimental efforts involve microjoule seed pulses and picosecond, millijoule pump pulses. To approach the ultimate goal of petawatt-exawatt laser powers, it is necessary to scale up the Raman scheme to nanosecond pump pulses that are available at the kilojoule energy level in

large laser systems. The first experimental demonstration employed a nanosecond pump pulse³ and an amplification of ~ 5 was achieved for a 2 μ J seed in a cold collisional plasma. A recent experiment with a 350 J, 1 ns pump showed an amplification of ~ 25 in a hot plasma where collisionless wave damping was dominant; however, with substantial attenuation of the seed pulse by the plasma due to spraying of the seed beam outside the collection cone.¹⁷ As discussed in Ref. 17, nanosecond pump pulses present more challenges in the Raman scheme. Due to the longer interaction time with the plasma, nanosecond pumps are more susceptible to instabilities, such as Raman scattering growing from thermal noise, which competes with the seed pulse, and filamentation instability which causes beam spray and degrades the optical quality of the amplified pulse. The heating of the plasma by the nanosecond-long pump will also likely lead to strong Landau damping of the plasma wave even in an optimized plasma amplifier. Studying Raman amplification in a high temperature plasma with strong Landau damping is also relevant to understanding the coupling of multiple laser beams in inertial confinement fusion experiments, where the individual beams undergo stimulated Raman scattering in the target interior, and the associated scatter can be further amplified as it crosses other beams upon exiting the target.^{18,19}

In this paper we present experimental results on a plasma amplifier pumped by nanosecond pulses, demonstrating an output energy of up to 14 mJ with an amplification of 2–20. It is found that the pump intensity should be kept below 1×10^{14} W/cm² to avoid beam spray. The attenuation of the seed pulse has been minimized in our experimental conditions. Particle-in-cell (PIC) and hydrodynamic simula-

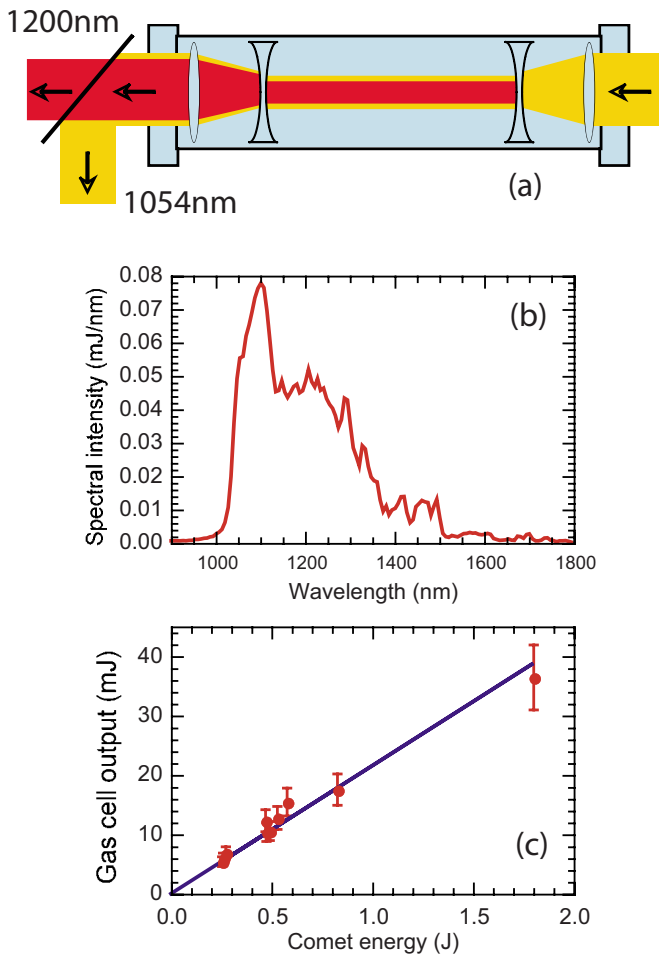


FIG. 1. (Color online) (a) Schematic of a Raman cell for seed pulse generation. (b) An output spectrum of the Raman gas cell filled with N_2O pumped by a 0.8 J COMET laser pulse. (c) Output energy of the gas cell vs COMET laser energy.

tions are also performed to help data interpretation. The paper is organized as follows. The generation of seed pulses is described in Sec. II. The experimental setup and results of filamentation study and amplification scaling are presented in Secs. III and IV, respectively. The simulation results are shown in Sec. V. Finally the summary is given in Sec. VI.

II. GENERATION OF SEED PULSES

Seed pulse generation is a critical step for Raman amplification. Since there is no pulsed laser available at relevant wavelengths, the seed pulse has to be created by redshifting a laser with the same wavelength as the pump. The wavelength shifting can be achieved by various methods, such as optical parametric processes,¹⁰ Raman crystals,¹³ or a Raman gas cell.¹⁷ For our experiment, we chose to use the Raman gas cell as it can handle J-level laser pulses with a reasonable efficiency. The schematic of the high-pressure cell is shown in Fig. 1(a). The windows were made of MgF_2 , which has a smaller nonlinear coefficient compared with other common optical materials. The thickness of the windows was chosen to sustain pressures up to 250 psi. It is necessary to keep the diameter of the incident beam large enough on the cell window to minimize the B-integral. Therefore, two pairs of

TABLE I. List of Raman gases for seed pulse generation.

Gas	Raman shift (cm^{-1})	Cross-section relative to σ_{N_2}	Order	Plasma density (10^{19} cm^{-3})
H_2	587	2.2	1	0.38
H_2	587	2.2	2	1.54
N_2O	1287	2.2	1	1.85
C_2H_6	993	1.6	1	1.10
C_3H_8	867	2.4	1	0.84
SO_2	1151	5.2	1	1.48
CO_2	1286	0.89	1	1.85

lenses were inserted inside the cell as a demagnification telescope to increase the intensity for Raman conversion. At the output of the cell, a beamsplitter that reflects $1.053 \mu\text{m}$ and transmits $>1.1 \mu\text{m}$ was set up to dump the unshifted beam. The output pulse was sent to an infrared (IR) spectrometer to measure its spectrum and a calorimeter for the energy. A list of Raman gases (from Refs. 20 and 21) and the corresponding plasma resonant density are given in Table I.

The pump beam for the cell was from the Compact Multipulse Terawatt (COMET) laser²² at the Jupiter Laser Facility (JLF) at Lawrence Livermore National Laboratory (LLNL). The pulse was chirped to ~ 5 ps in order to minimize the B-integral in the cell. The output redshifted pulse was found to have a similar duration as the pump pulse. A laser energy up to 1.8 J at 1054 nm was employed to pump the cell. Among the gases listed in Table I, H_2 , N_2O , C_2H_6 , and C_3H_8 were tested for the conversion efficiency at the redshifted wavelength ~ 1200 nm. It is found that N_2O provides the highest spectral intensity at 1200 nm. A spectrum of the N_2O -filled gas cell pumped by a 0.8 J COMET laser pulse is displayed in Fig. 1(b). The output energy of the gas cell after the beamsplitter is approximately proportional to the input COMET laser energy with a conversion efficiency of $\sim 2\%$, as shown in Fig. 1(c). Up to ~ 40 mJ was obtained although the energy was distributed in a wide spectrum. In future experiments a small gas cell will be added to seed the Raman conversion in order to improve the efficiency.

III. ANGULAR SPREAD OF THE OUTPUT PULSE

An experiment was carried out at JLF to study the beam quality of the output pulse in a plasma, where Raman amplification occurs. The 1 ns Janus laser²³ was employed as the pump pulse and the seed pulse was created using the 5 ps COMET laser, as described above. Earlier experiments indicated a significant attenuation of the seed due to beam spray out of the detector collection cone. In this experiment we study the dependence of beam spray on pump intensity in an exactly counterpropagating geometry. This geometry has the advantage that the interaction region of the two beams is extended to 3 mm even with a $200 \mu\text{m}$ spot size of the pump beam, which allows access to high pump beam intensity. The experimental setup is illustrated in Fig. 2. The Janus beam was smoothed with a $200 \mu\text{m}$ phase plate and focused to the center of a helium gas jet. The plasma, created by the pump itself through ionization of the gas, was ~ 3 mm long

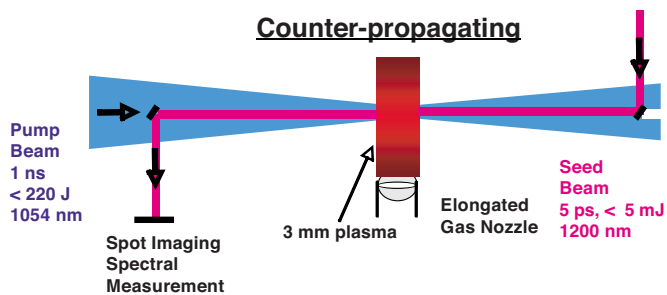


FIG. 2. (Color online) Experimental setup of counterpropagation geometry.

and the pump intensity was above half of its peak value over this entire region. A small (0.5 in. diameter) concave mirror was inserted in the exiting Janus beam to direct and focus the seed pulse to counterpropagate with the pump. The corresponding center portion of the pump was also blocked upstream to allow a small pickoff mirror to be inserted to direct the amplified seed to detectors, while minimizing damage to both small mirrors. The blocked area is $\sim 50\%$ of the total beam area. The energy loss due to the center blocking was not an issue for this experiment, and the hollow beam profile did not significantly affect the focus of the pump since a phase plate was applied. A similar 0.5 in. mirror was set up on the opposite side to collect the pulse after the interaction. The output beam was sent to an IR one-dimensional (1D) photoarray, which was covered by a bandpass filter at 1200 nm with a bandwidth of 70 nm. The surface of the output 0.5 in. mirror was imaged onto the photoarray to measure the angular spray of the transmitted seed pulse. The gas jet backing pressure was set to 1200 psi. The He plasma was fully ionized even with half of the lowest pump energy. Therefore in our experiment the plasma density was not affected by pump intensity but mainly depended on the gas pressure. According to the measurements in Ref. 17, the plasma density should be near 10^{19} cm^{-3} . The seed pulse was synchronized to the middle of the 1 ns pump at the gas jet using a fast photodiode with a time response of 30 ps.

Figure 3 shows the measured angular profiles of the output beam at three pump intensities, as well as the seed beam itself without plasma nor the pump ("seed only"). The profile is normalized to the peak of the seed only case. It is clear that the beam quality deteriorates as the pump intensity increases as evidenced by the transmitted seed spraying out to angles well outside its incident angular profile, which is contained within a cone of angle $\pm 1.2^\circ$. At $I_{\text{pump}} = 0.8 \times 10^{14}\text{ W/cm}^2$, the transmitted seed pulse has a similar profile to that of the incident one albeit with $\sim 2\times$ attenuation. At $1.6 \times 10^{14}\text{ W/cm}^2$ the transmitted profile has broad wings extending at least to the edge of the measurement cone ($\pm 3.5^\circ$) with only a small narrow feature in the center representing a small fraction of the light that is not significantly scattered. Finally when the I_{pump} increases to $2.4 \times 10^{14}\text{ W/cm}^2$, the profile is completely flattened and the transmission drops down to less than 10%, indicating a large beam spray well beyond the measurement cone. These features are consistent with the pump beam filamentation causing angular deflection of the seed. Scattering of one spatial frequency component of

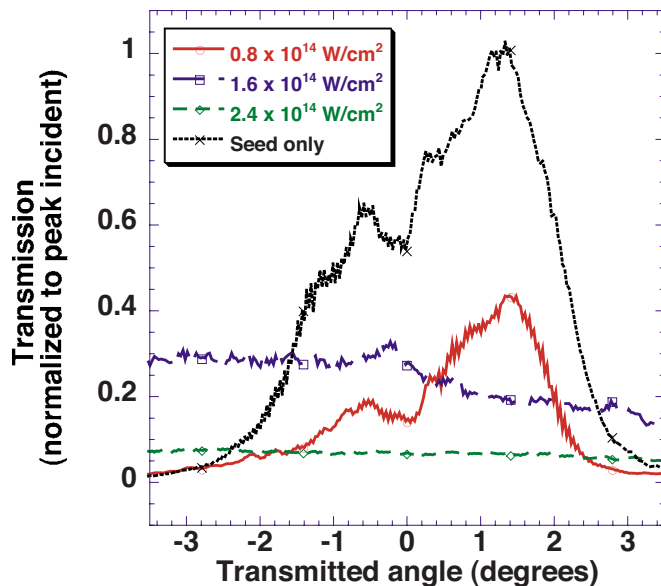


FIG. 3. (Color online) Angular profiles of the seed itself and output pulses at three pump intensities in exact counterpropagation geometry.

the pump by a plasma wave produced by a different spatial component can also cause the amplified beam to have larger angular divergence than the incident seed; however, the scattering is not coherent with any of the incident seed spatial frequencies. Therefore, when the amplification is small there is not much energy in this scattering. The measurement with a seed at a different frequency was carried out in an earlier experiment¹⁷ using an 1124 nm line in a plasma that was resonant at 1200 nm. It was found that the transmission of the seed into the detector was greatly reduced consistent with the beam spray occurring even to beams that are not Raman amplified. Therefore we think that scattering by different angular harmonics of the pump could also occur but the observations we report seem more consistent with pump filamentation.

Onset of filamentation seeded by highest intensity speckles in the incident beam is expected as the pump intensity increases over the range shown in Fig. 3. To show this we estimated the threshold of filamentation using the method in Ref. 24. The intensity distribution of a laser spot with a flat-top-envelope phase plate is given by $(1+I/\bar{I})\exp(-I/\bar{I})$, where \bar{I} is the average intensity. There is 4% of power contained in speckles which have an intensity of $\times 5\bar{I}$. These speckles, with a typical size given by the diffraction limit of the entire optic, clearly play a critical role in seeding the filamentation instability. The threshold of ponderomotive filamentation is given by $(v_0/v_{\text{th}})^2(n_e/n_c)(L/\lambda)^2 > 1$,²⁴ where v_0 is the oscillatory velocity of an electron in the laser field, v_{th} is the electron thermal velocity, n_e is the plasma density, n_c is the critical density, L is the speckle size, and λ is the laser wavelength. Given our experimental conditions, $\lambda = 1.053\text{ }\mu\text{m}$, $n_e \sim 1 \times 10^{19}\text{ cm}^{-3}$, $L \sim 10\text{ }\mu\text{m}$, and electron temperature $T_e \sim 200\text{ eV}$,¹⁷ the threshold of the speckle intensity is estimated to be $7.5 \times 10^{14}\text{ W/cm}^2$. The average intensity is $5\times$ lower, i.e., $1.5 \times 10^{14}\text{ W/cm}^2$, which assuming an exponential distribution of speckle intensities, indi-

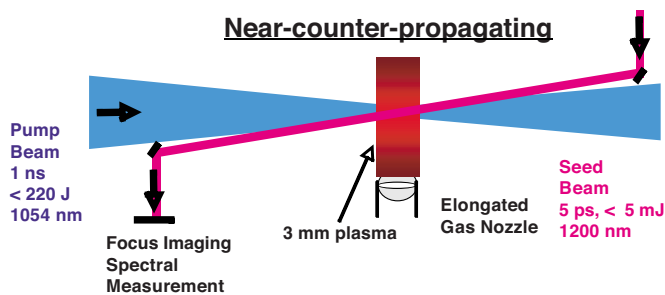


FIG. 4. (Color online) Near-counterpropagating setup.

icates that observed beam spray occurs when more than a few percent of the beam energy is above the threshold intensity for filamentation. When this condition is surpassed, it can be seen from the data in Fig. 3 that filaments in the pump beam are perturbing the plasma density sufficiently to modify the transmitted profile of the seed beam and cause an apparent low transmission of the seed due to large beam spray outside the collection optics. These angular profiles represent the amplitudes of the output pulse, while the focusability will be affected by both amplitudes and the phases. The focusability of the amplified pulse with existing random density inhomogeneities has been studied in numerical simulations,⁸ and a simple expression is given for the plasma length limit in order to maintain good focusability, which is independent of the pump intensity. Our measurements show that pump filamentation is one source for generating the density inhomogeneities. Therefore the pump intensity should be kept below the filamentation threshold.

IV. SCALING OF AMPLIFICATION

Having established the beam and plasma conditions that will allow high focal quality beams to be amplified, we performed a second series of experiment using a near counter-propagating setup (Fig. 4) to avoid the complication of inserting a mirror into the pump beam in the counterpropagating geometry. The results discussed in Sec. III indicate that amplification of high focal quality beams can be best achieved at intensities much lower than were used in Ref. 17. Therefore we can increase the spot size from 200 to 500 μm , while maintaining the needed intensity and the 3 mm interaction length. The seed pulse was directed to the gas jet by a mirror located outside of the pump beam. The crossing angle between the 5 ps seed and the 1 ns pump was 11°. The phase plate for the pump was changed to one with a 500 μm spot to allow more energy, while keeping the pump intensity below the filamentation threshold. Part of the amplified pulse was split out and sent into an IR spectrometer for measuring its spectrum, and the rest was directed to the same calibrated IR photoarray covered by the 1200 nm filter for beam profile measurements. In this experiment, the photoarray imaged the focus of the seed pulse, which had a full width at half maximum (FWHM) $\sim 500\ \mu\text{m}$. The effective interaction length in this near-counterpropagating geometry is $\sim 3\ \text{mm}$, which matched the gas jet length.

The beam profiles of the amplified pulse (pump+seed), the seed pulse itself (seed only) and the thermal Raman

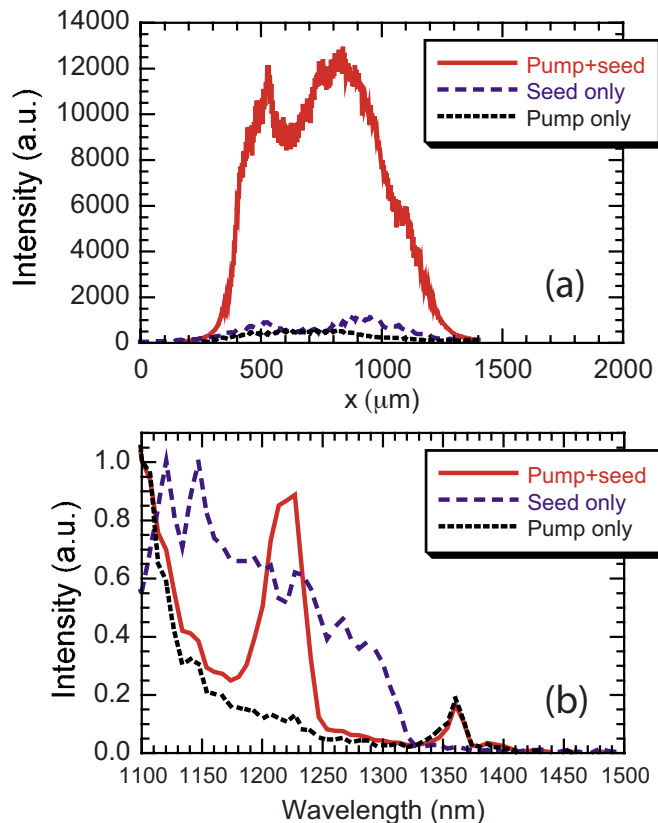


FIG. 5. (Color online) Output beam profiles (a) and normalized spectra (b) of amplified pulse (pump+seed), the seed pulse itself (seed only), and the thermal Raman (pump only). (a) shows the relative magnitudes of transmitted energy density, while in (b) the spectra are normalized by their own maxima to allow direct comparison.

(pump only) obtained by the photoarray are shown in Fig. 5(a). The energies of the pump and the seed were 233 J and 3.5 mJ, respectively, corresponding to intensities of 1.2×10^{14} and 8.5×10^{10} W/cm^2 (FWHM). The thermal Raman was slightly weaker than the seed pulse. When the pump and the seed were both present, the output beam showed enhancement with a profile similar to that of the input seed, demonstrating that the optical quality of the pulse was maintained through Raman amplification in the plasma. The spectra of the amplified pulse, the seed and the thermal Raman are shown in Fig. 5(b). Each spectrum was normalized by its own maximum so that the spectral distribution can be compared at the same level. A resonant peak is clearly seen at 1220 nm with a FWHM $\sim 40\ \text{nm}$, which is much narrower than the seed spectrum. Therefore, only a small portion of the seed pulse was amplified. For the shot shown in Fig. 5, the energy of the seed pulse inside the resonant bandwidth was $\sim 1.1\ \text{mJ}$. For the data hereafter the seed energy refers to the energy within this bandwidth.

The photoarray was operated in the linear response regime so that the counts of the profile were proportional to the beam energy. The energy response of the photoarray was calibrated using the seed pulse and a calibrated calorimeter. The amplification was thus calculated as the ratio of the integrated beam profile of the pump+seed (with the thermal Raman signal subtracted) to that of seed only. Because the actual beam profile was two-dimensional and the photoarray

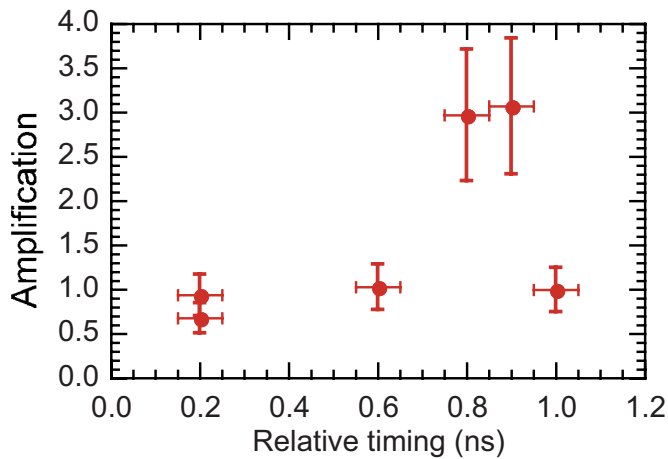


FIG. 6. (Color online) Amplification vs relative timing between the pump and the seed.

only sampled a lineout across the center, the total beam energy was calculated assuming circular symmetry. The profile was not exactly symmetric, which contributed to the error bar in the figures in this paper. Because the photoarray was covered by the 1200 nm bandpass filter, the amplification refers to the energy within the 70 nm bandwidth of the filter. The data in Fig. 5(a) show an amplification of 11.

The timing between the pump and the seed was also varied to optimize the amplification and plasma conditions. The results with a 180 J pump and a 1.5 mJ seed are plotted in Fig. 6. The intensities of the pump and the seed were 8×10^{13} and 1.3×10^{11} W/cm² at FWHM, respectively. As shown in Fig. 6, an amplification of ~ 3 was observed during the timing scan. The lower amplification compared with the result in Fig. 5 is due to the lower pump intensity during timing scan. The time window for amplification for wavelengths near 1220 nm was ~ 0.2 ns and occurred in the later portion of the pump when plasma was hottest. This indicates that the heating of the plasma by the high intensity nanosecond pump does not prevent amplification, which is an important result for developing high energy Raman amplifiers in which the plasma temperature is high and Landau damping of the plasma wave due to heating is large. In addition, the transmission of the seed pulse outside the amplification time window was close to 100%, indicating that the Raman amplification was not interfered by absorption of the seed pulse. The narrow time window for the amplification is not fully understood, probably due to changing plasma conditions during the pump pulse since the plasma is created by the pump itself. In future experiments a suite of diagnostics will be added to further study the plasma conditions.

The amplification as a function of pump and seed intensities is shown in Fig. 7. At a pump intensity of 1.2×10^{14} W/cm², the output energy reaches 4.8, 12.1, 12.7, and 13.9 mJ for seed energies of 0.24, 1.1, 1.7, and 6.3 mJ, respectively, corresponding to amplifications of 20, 11, 7.6, and 2.2. There was a factor of 2–3 shot-to-shot fluctuation in the amplified pulse energy. The data in Fig. 7(a) represent the maximum output energy observed. Figure 7(b) shows that when the pump intensity is varied from 5.7×10^{13} ,

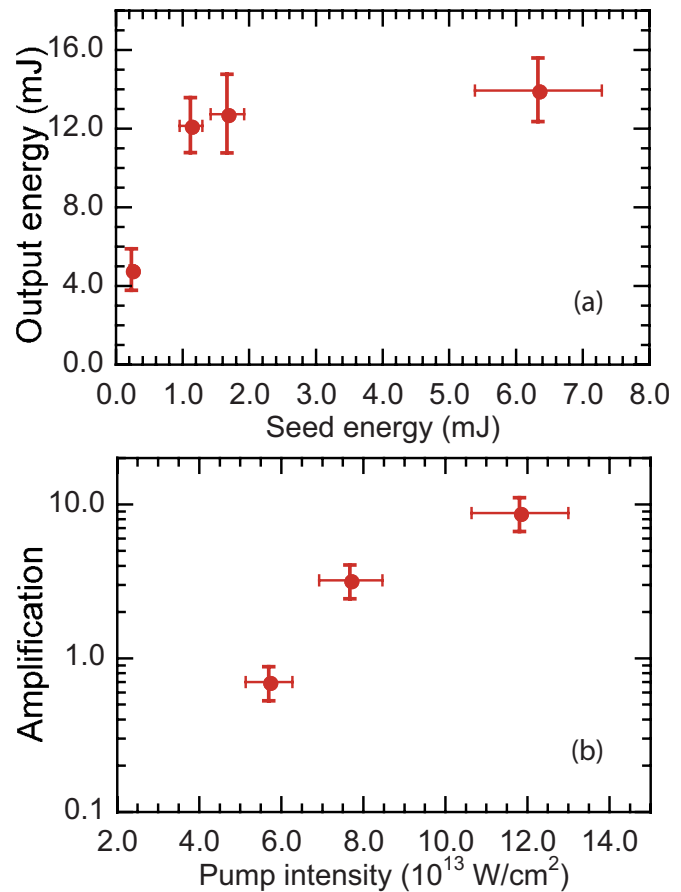


FIG. 7. (Color online) (a) Observed maximum output energy as a function of seed energy at a pump intensity of 1.2×10^{14} W/cm². (b) Amplification of a 1.7 mJ seed vs the pump intensity.

7.7×10^{13} , to 1.2×10^{14} W/cm², the amplification is 0.7, 3.2, and 7.6 for a 1.7 mJ seed. If the Raman process is in the linear regime, the output energy should be proportional to the seed energy and the amplification grows exponentially with the pump intensity. The data points are consistent with the onset of nonlinearity in the amplification in the highest energy cases. In particular, in the pump intensity scan, the reduction in amplification below the exponential line fit to the first two points with lower pump intensities (those below 1×10^{14} W/cm²) could be explained by the onset of beam spray, as discussed in Sec. III, but also could be produced by a different linear response in the different plasma conditions at higher pump intensity. The seed energy scan in Fig. 7(a) showed a clearer nonlinearity at higher seed energies, where the output energy is seen to saturate. One possible reason causing the saturation is variation in seed quality as the pump energy for the Raman gas cell increases. However both the seed spectrum and the beam profile were similar to those low energy shots, and the gain of the Raman cell is still linear for the highest seed energy, as seen in Fig. 1(c). Therefore we did not find any evidence for deterioration of the seed quality. We think that the amplification saturation indicates that the plasma wave is not scattering in proportion to the ponderomotive force driving it as it should if its response is linear. The scan of seed energy allows the wave drive to be varied without affecting the other nonlinear processes as a

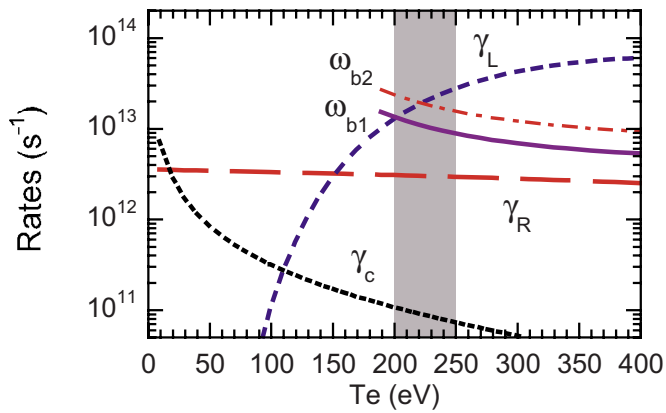


FIG. 8. (Color online) Various rates as a function of temperature.

result of variations in the pump intensity. The mechanism that saturates the amplification as the seed energy increases is discussed in Sec. V together with simulation results.

V. DISCUSSIONS AND PIC SIMULATIONS

To understand the experimental results it is helpful to estimate the rates of various processes in the laser-plasma interaction. These rates, shown in Fig. 8 as a function of temperature, are calculated using the standard formulae in Refs. 25 and 26. The weak dependence of linear Raman growth rate (γ_R) on temperature is due to the temperature correction in plasma frequency based on Bohm–Gross relation. As the temperature rises up, collision rate (γ_c) decreases and Landau damping rate (γ_L) increases substantially as expected. According to hydrodynamic simulations using HYDRA,¹⁷ the temperature of the He plasma created by the ~ 200 J, 1 ns pump reaches 200–250 eV as marked by the shaded area. At such a high temperature collisions are negligible and Landau damping dominates over Raman growth. As a result, the plasma wave can hardly grow unless strongly driven by the interference between the pump and the seed pulses. Another important rate is the electron bounce frequency (ω_b) in the Langmuir wave potential, which is defined as $\omega_b^2 = ek_p E_p / m$ (Ref. 25) (e is the electron charge, k_p and E_p are the wave vector and electric field of the plasma wave, and m is the electron mass). The plasma wave amplitude can be normalized as $a_p = eE_p / (mc\sqrt{\omega_0\omega_p})$, where ω_0 is the pump frequency, ω_p is the plasma wave frequency, and c is the speed of light. In the strong damping regime ($\gamma_L \gg \gamma_R$) with negligible pump depletion, $a_p \approx (\gamma_R / \gamma_L) a_{\text{seed}}$ (a_{seed} is the normalized amplitude of vector potential of the seed). Therefore, the plasma wave becomes localized inside the seed pulse. Given $k_p \sim 2k_0$ in a counterpropagation geometry (k_0 is the wave vector of the pump), the bounce frequency is then $\omega_b^2 \sim 2\omega_0\sqrt{\omega_0\omega_p}\gamma_R a_{\text{seed}} / \gamma_L$. Two bounce frequencies are plotted in Fig. 8, ω_{b1} for a 1.5 mJ seed and ω_{b2} for a 15 mJ seed. It can be seen that as the seed amplitude increases, the bounce frequency becomes comparable with the Landau damping rate, indicating that particle trapping may play a role in the evolution of the plasma wave. It should be noted that in the strong damping regime the

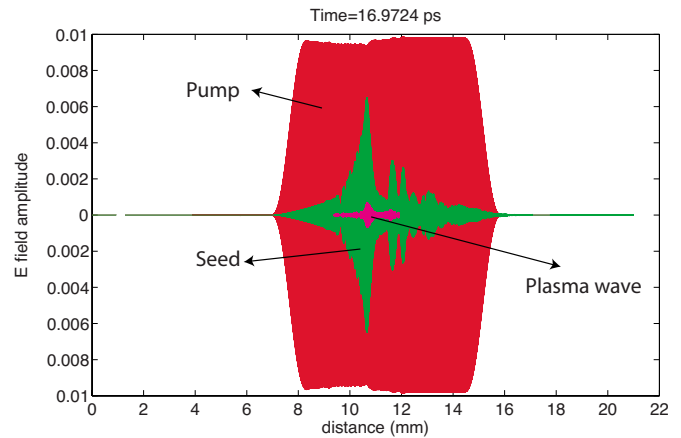


FIG. 9. (Color online) A snapshot of the pump, the seed, and the plasma wave in the PIC simulation.

effective Raman growth rate will be lower than the linear growth rate estimated here.²⁷ Nonetheless the correction will not change the relative importance of the rates.

To gain an insight into the dynamics of this three-wave interaction, we performed 1D PIC simulations using the fully kinetic code OSIRIS.²⁸ The PIC simulation was downscaled because with a 3-mm-long plasma, only 20 ps of the pump pulse actually interacts with the seed in a counterpropagating geometry. The simulation was set up as follows. A 3 mm plasma slab is located in the middle of the simulation box as a density step profile with vacuum regions on both sides. The plasma temperature is 200 eV, as obtained from hydrodynamic simulations. The density is $1.1 \times 10^{19} \text{ cm}^{-3}$ at which the plasma frequency with thermal correction satisfies the resonant condition with the pump and the seed. The pump intensity of $1.2 \times 10^{14} \text{ W/cm}^2$ ($a_{\text{pump}0} = 0.0098$) is prescribed throughout the flat region with the scaling of energy in 20 ps that gives the same intensity as in 1 ns for a 500 μm FWHM spot. The seed has a Gaussian longitudinal profile with 5 ps pulse width. For a seed energy of 1.5 mJ and 500 μm FWHM spot, the peak intensity is $2.9 \times 10^{11} \text{ W/cm}^2$ and $a_{\text{seed}0} = 0.00055$. Please note that although intensities are calculated assuming transverse Gaussian spot sizes, the simulation is 1D so the lasers are infinite plane waves. Therefore no transverse effects such as filamentation, diffraction, and focusing of the pump and seed beams are modeled and hence we expect the amount of gain to be different in the simulation from what is measured in an experiment under the same plasma conditions. In addition, in the experiment the seed interacts with the pump at 11° off of the direct counterpropagating direction and this is not modeled by the simulation. Therefore, the PIC simulations are intended to provide qualitative insight into physical processes rather than to quantitatively fit the data.

Figure 9 displays a snapshot of the three-wave interaction. The electric fields of the pump and the seed are differentiated by their directionality through Poynting vector. It is obvious that the envelope of the plasma wave resembles that of the seed pulse, consistent with the strong damping regime as described above. Figure 10 shows the simulated time his-

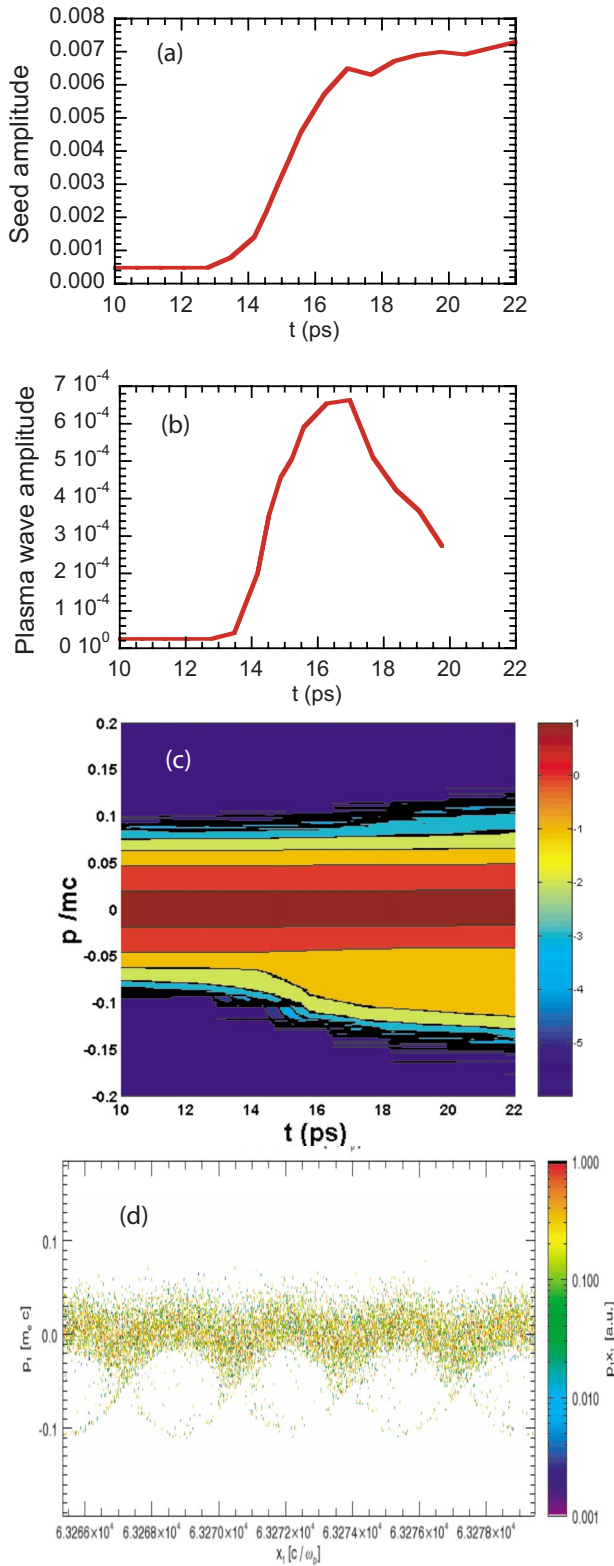


FIG. 10. (Color online) Temporal evolution of seed amplitude (a), plasma wave amplitude (b) and electron distribution function $f_e(v)$ (c) from PIC simulations. The contour map of $f_e(v)$ is on log scale. (d) Electron phase space at $t=17$ ps, showing the vortices of trapped particles.

tory of the peak electric field amplitude of the seed pulse, the plasma wave amplitude and the velocity distribution of electrons, respectively. The seed amplitude is normalized by $m\omega_0 c/e$ and the plasma wave amplitude is normalized by

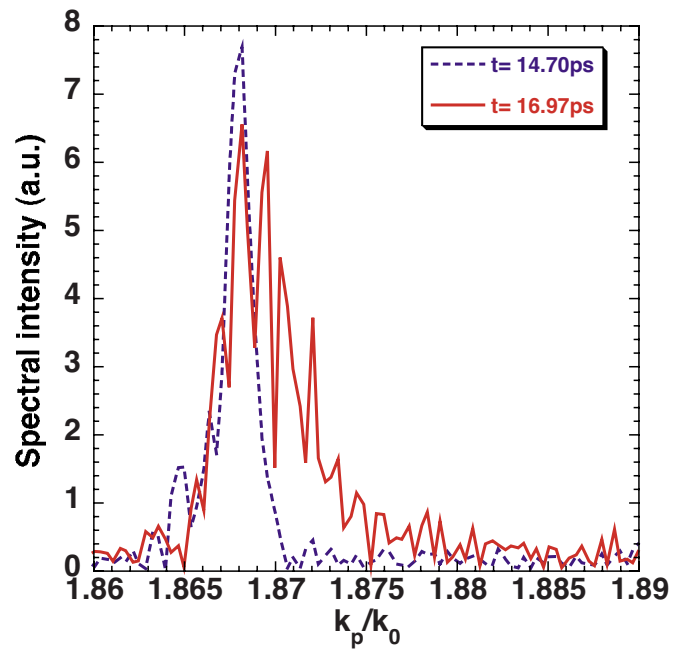


FIG. 11. (Color online) The k spectra of the plasma wave at $t=14.70$ ps and $t=16.97$ ps, showing the broadening and shift of the plasma wave number.

$m\sqrt{\omega_0\omega_p}c/e$. As the seed interacts with the pump in the plasma, its amplitude grows near-exponentially for about 3 ps and then saturates at ~ 0.007 . The amplification in these 1D simulations is ~ 100 , which is higher than what was observed in experiments. It is clear that the saturation of seed amplification is coincident with the level-off of the plasma wave amplitude [Fig. 10(b)]. The evolution of electron velocity distribution function shown in Fig. 10(c) indicates that flattening of velocity distribution function near $v=v_{ph} \approx 0.07c$ ($v_{ph}=\omega_p/k_p$ is the phase velocity of the plasma wave), which is a signature of particle trapping, occurs immediately before the saturation of amplification. A clearer evidence of particle trapping is the appearance of vortices in the electron phase space, which is shown in Fig. 10(d) for $t=17$ ps. The flattening of the electron distribution function should result in the reduction in the Landau damping rate,²⁹ which would increase the wave coupling. However we observed the opposite tendency. It is also known that the non-linear frequency shift of the plasma wave could detune the resonance and reduce the scattering.³⁰ Figure 11 shows the k spectra of the plasma wave in the PIC simulations at $t=14.70$ ps (before saturation) and $t=16.97$ ps (onset of saturation). It can be seen that the k spectrum is broadened and shifted compared with that at an earlier time, which might explain the saturation of the amplification.

To overcome such a saturation a shorter seed pulse can be employed because the sharper front of the pulse can grow before particle trapping occurs. Shown in Fig. 12 are the simulation results with the same parameters, as in Fig. 10 except the seed pulse is only 0.5 ps long (the initial amplitude is the same). In this case the seed pulse continues to

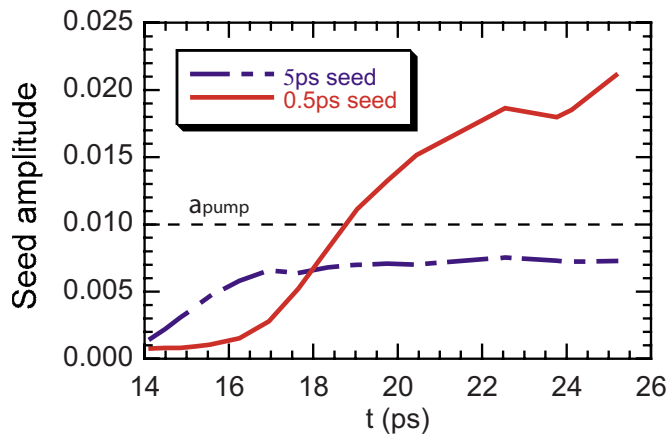


FIG. 12. (Color online) Evolution of seed amplitude for a 5 and 0.5 ps seed. The dashed line marks the amplitude of the pump.

grow without saturation in the 3 mm plasma. The amplification reaches ~ 1000 times and the amplitude of the amplified pulse exceeds that of the pump, indicating a power gain. These promising simulation results provide important guidance for future experiments.

VI. SUMMARY

To summarize, we have demonstrated Raman amplification with a nanosecond pump pulse in a relatively hot plasma where Landau damping dominates. An amplification of up to 20 and a maximum output energy of 14 mJ have been achieved. Saturation of amplification is observed as the seed energy increases. PIC simulations indicate that the saturation is consistent with particle trapping as the mechanism. This saturation effect may be important for minimizing Raman backscattering loss of the multiple crossing beams used for the ignition of fusion reactions by indirect drive.¹⁹ In addition the PIC simulations suggest that a shorter seed pulse could be helpful to overcome the observed saturation and allow more efficient Raman amplification and compression of laser pulses.

ACKNOWLEDGMENTS

We wish to thank JLF Team for laser operation and G. Freeze for technical support. We also thank W. B. Mori and the OSIRIS consortium for use of the OSIRIS code. This work was performed under the auspices of the U.S. Department of Energy by LLNL under Contract No. DE-AC52-07NA27344.

- ¹G. Shvets, N. J. Fisch, A. Pukhov, and J. Meyer-ter-Vehn, *Phys. Rev. Lett.* **81**, 4879 (1998).
- ²V. M. Malkin, G. Shvets, and N. J. Fisch, *Phys. Rev. Lett.* **82**, 4448 (1999).
- ³Y. Ping, I. Geltner, N. J. Fisch, G. Shvets, and S. Suckewer, *Phys. Rev. E* **62**, R4532 (2000).
- ⁴D. S. Clark and N. J. Fisch, *Phys. Plasmas* **10**, 3363 (2003).
- ⁵N. A. Yampolsky, N. J. Fisch, V. M. Malkin, E. J. Valeo, R. Lindberg, J. Wurtele, J. Ren, S. Li, A. Morozov, and S. Suckewer, *Phys. Plasmas* **15**, 113104 (2008).
- ⁶A. A. Balakin, G. M. Fraiman, and N. J. Fisch, *JETP Lett.* **80**, 12 (2004).
- ⁷V. M. Malkin and N. J. Fisch, *Phys. Plasmas* **8**, 4698 (2001); **10**, 2056 (2003); **12**, 044507 (2005).
- ⁸A. A. Solodov, V. M. Malkin, and N. J. Fisch, *Phys. Plasmas* **10**, 2540 (2003).
- ⁹R. L. Berger, D. S. Clark, A. A. Solokov, E. J. Valeo, and N. J. Fisch, *Phys. Plasmas* **11**, 1931 (2004).
- ¹⁰Y. Ping, I. Geltner, A. Morozov, N. J. Fisch, and S. Suckewer, *Phys. Rev. E* **66**, 046401 (2002).
- ¹¹Y. Ping, I. Geltner, and S. Suckewer, *Phys. Rev. E* **67**, 016401 (2003).
- ¹²Y. Ping, W. Cheng, and S. Suckewer, *Phys. Rev. Lett.* **92**, 175007 (2004).
- ¹³W. Cheng, Y. Avitzour, Y. Ping, S. Suckewer, N. J. Fisch, M. S. Hur, and J. S. Wurtele, *Phys. Rev. Lett.* **94**, 045003 (2005).
- ¹⁴M. Dreher, E. Takahashi, J. Meyer-ter-Vehn, and K. J. Witte, *Phys. Rev. Lett.* **93**, 095001 (2004).
- ¹⁵J. Ren, W. Cheng, S. Li, and S. Suckewer, *Nat. Phys.* **3**, 732 (2007); J. Ren, S. Li, A. Morozov, S. Suckewer, N. A. Yampolsky, V. M. Malkin, and N. J. Fisch, *Phys. Plasmas* **15**, 056702 (2008).
- ¹⁶C.-H. Pai, M.-W. Lin, L.-C. Ha, S.-T. Huang, Y.-C. Tsou, H.-H. Chu, J.-Y. Lin, J. Wang, and S.-Y. Chen, *Phys. Rev. Lett.* **101**, 065005 (2008).
- ¹⁷R. K. Kirkwood, E. Dewald, C. Niemann, N. Meezan, S. C. Wilks, D. W. Price, O. L. Landen, J. Wurtele, A. E. Charman, R. Lindberg, N. J. Fisch, V. M. Malkin, and E. O. Valeo, *Phys. Plasmas* **14**, 113109 (2007).
- ¹⁸R. K. Kirkwood, Y. Ping, N. Meezan, S. C. Wilks, P. Michel, E. Williams, D. Clark, L. Suter, N. J. Fisch, E. J. Valeo, V. Malkin, J. Wurtele, T. L. Wang, and C. Joshi, "Observation of amplification of light by Langmuir waves and its saturation on the electron kinetic timescale" (unpublished).
- ¹⁹R. K. Kirkwood, D. S. Montgomery, B. B. Afeyan, J. D. Moody, B. J. MacGowan, C. Joshi, K. B. Wharton, S. H. Glenzer, E. A. Williams, P. E. Young, W. L. Kruer, K. G. Estabrook, and R. L. Berger, *Phys. Rev. Lett.* **83**, 2965 (1999).
- ²⁰D. G. Fouce and R. K. Chang, *Appl. Phys. Lett.* **20**, 256 (1972).
- ²¹W. R. Fenner, H. A. Hyatt, J. M. Kellam, and S. P. S. Porto, *J. Opt. Soc. Am.* **63**, 73 (1973).
- ²²J. Dunn, J. Nilsen, A. L. Osterheld, Y. Lin, and V. N. Shlyaptsev, *Opt. Lett.* **24**, 101 (1999).
- ²³W. L. Kruer, *Phys. Fluids B* **3**, 2356 (1991).
- ²⁴E. A. Williams, *Phys. Plasmas* **13**, 056310 (2006).
- ²⁵W. L. Kruer, *Physics of Laser Plasma Interactions* (Addison-Wesley, Reading, MA, 1988).
- ²⁶J. D. Huba, *NRL Plasma Formulary* (Naval Research Laboratory, Washington, DC, 2000).
- ²⁷P. Mounaix and D. Pesme, *Phys. Rev. E* **55**, 4653 (1997).
- ²⁸R. A. Fonseca, L. O. Silva, R. G. Hemker, F. S. Tsung, V. K. Decyk, W. Lu, C. Ren, W. B. Mori, S. Deng, S. Lee, T. Katsouleas, and J. C. Adam, in *International Conference on Computational Science*, Lecture Notes in Computer Science Vol. 2331, edited by P. M. A. Sloot (Springer-Verlag, Berlin, 2002), pp. 342–351.
- ²⁹T. O'Neil, *Phys. Fluids* **8**, 2255 (1965).
- ³⁰G. J. Morales and T. O'Neil, *Phys. Rev. Lett.* **28**, 417 (1972).